

Development of alkali activated cements and concrete mixture design
with high volumes of red mud

Non Peer-reviewed author version

Krivenko, Pavel; Kovalchuk, Oleksandr; Pasko, Anton; CROYMANS-PLAGHKI, Tom; Hutt, Mikael; Lutter, Guillaume; VANDEVENNE, Niels; SCHREURS, Sonja & SCHROEYERS, Wouter (2017) Development of alkali activated cements and concrete mixture design with high volumes of red mud. In: CONSTRUCTION AND BUILDING MATERIALS, 151, p. 819-826.

DOI: 10.1016/j.conbuildmat.2017.06.031

Handle: <http://hdl.handle.net/1942/24843>

Development of alkali activated cements and concrete mixture design with high volumes of red mud

Pavel Krivenko^a, Oleksandr Kovalchuk^b, AntonPasko^c, Tom Croymans^d,
Mikael Hult^e, Guillaume Lutter^f, Niels Vandevenne^g, Sonja Schreurs^h,
Wouter Schroeyersⁱ

^{a, b, c} V.D.Glukhovsky Scientific Research Institute of Binders and Materials, Kiev
National University of Construction and Architecture, Vozdukhoflotsky pr.,
31 Kiev 03037 Ukraine

^{d, g, h, i} NuTeC, CMK, Nuclear Technology - Faculty of Engineering Technology
Hasselt University, Agoralaan building H, B-3590 Diepenbeek, Belgium

^{e, f} JRC-Geel, Retieseweg 111, 2440 Geel, Belgium

^a *pavlo.kryvenko@gmail.com*; ^b *kovalchuk_oyu@knuba.edu.ua*; ^c *ua.pasko@gmail.com*;
^d *tom.croymansplaghki@uhasselt.be*; ^e *Mikael.HULT@ec.europa.eu*;
^f *Guillaume.LUTTER@ec.europa.eu*; ^g *niels.vandevenne@uhasselt.be*;
^h *sonja.schreurs@uhasselt.be*; ⁱ *wouter.schroeyers@uhasselt.be*

Abstract

Dedicated cement compositions were formulated to enable the incorporation of large volume fractions of red mud in alkali activated cements, taking into account the role of the aluminosilicate phase in the processes of hydration and hardening. High volume red mud alkali activated cements were synthesized using a proper combination of red mud, low basic aluminosilicate compounds with a glass phase (blast-furnace slag) and additives selected from high-basic Ca-containing cements with a crystalline structure (Portland cement). Compressive strength of the cements under study is 30-60 MPa (tested in mortar). The microstructure of the hardened cement paste and the role of red mud in the structure formation process were investigated. In addition to the use of red mud in cement, its use as an aggregate in concrete was studied to enable the use of larger quantities in the final concrete. In concrete road bases, the use of red mud can reach even 90% by mass. Since enhanced concentrations of naturally occurring radionuclides can be present in red mud this aspect was investigated to make sure that these materials are safe to use from a radiological point of view.

Highlights

- High volume red mud alkali activated cements and concretes have high strength.
- Hydration products are low-basic CSHs and alkaline ferro- and aluminosilicates.
- From radiological safety, concretes with 90% can be used for road construction.

Keywords: alkali activated cements, concrete, red mud, structure formation

1. Introduction

The Bayer process is a principal commercial technology to purify bauxite and produce alumina (Al₂O₃). During the Bayer process red mud is produced as a major

by-product. It can be a hazardous material owing to its alkalinity but also because of its enhanced levels of natural occurring radionuclides. A typical plant produces up to twice as much red mud as alumina. Today, over 2.7 billion tons is available worldwide [Liu and Li, 2015]. Disposal costs of red mud can add up to 5% of alumina production costs and it also introduces risks to the environment. Therefore, a lot of effort is dedicated to find suitable applications for use of the large reserves of red mud that are available worldwide. The use of red mud on a large scale in the production of construction materials can be a commercially viable option. Several studies have investigated the application of red mud as an additive for building materials [Sglavo et al, 2000; Hairi, 2015; Pontikes et al, 2007; Tsakiridis, et al, 2004; Pascual et al, 2009; Ye et al, 2014]. In the preparation of special cements from red mud the added quantity of red mud is usually less than 5% [Manfroi et al., 2014; Singh et al., 1997; Pontikes et al, 2007; Tsakiridis et al., 2004]. Alkaline activation allows to considerably increase the quantities of red mud incorporated both in cements and concretes without a decrease of their physico- mechanical characteristics [Pan et al 2003, Pan et al 2002, Ke et al, 2014; Klauber et al, 2011; He et al, 2012; Zhang et al, 2014; Zhang et al, 2010; Kumar et al, 2013; Dimas et al, 2009; Hajjajia et al, 2013. Vukcevic et al, 2013; Komnitsas et al, 2009; He et al, 2013 Bošković et al, 2013; Ke et al, 2015]. The limited incorporation levels of red mud can be explained by the fact that such important factors such as the chemical composition of constituent materials, the state of structure and the type of alkaline activator have not been optimized. These factors, according to Glukhovsky (1992) and Krivenko (1985) are important with regard to the formation of alkaline and alkaline- alkali earth phases which eventually determine the properties of the resulting cement stone.

An option to use large percentages of red mud is to chemically and thermally convert them to inorganic polymer mortar [Hertel et al., 2016]. The mayor disadvantage of this process is that it is very energy intensive. However, in order to develop an industrially viable option it is crucial to study options for reuse that do not require such an energy intensive pretreatment step.

Red mud has a low hydraulic activity. Any cement composition containing red mud should therefore be modified by activating additives, such as amorphous silica, which do not contain calcium. The main goal of the current research is to optimize the formation process of red mud based alkali activated cements. In order to achieve this goal, it is important to control the alkaline medium (alkalinity) and the presence of oxides, such as CaO , Al_2O_3 , SiO_2 , Fe_2O_3 and others in the active form. The alkalinity and oxides are required for synthesis of proper hydration products—mineral substances of alkaline aluminosilicate composition. As a rule, these substances act as structure-forming elements not only during the formation of solid rocks in nature, but in ancient concretes as well. Analcime, an alkaline aluminosilicate hydrate composed of Na_2O , Al_2O_3 , SiO_2 , H_2O , is formed in ancient cements and acts as a so-called "eternal" bond. Specific features of ancient cements, distinguishing them from contemporary Portland cements, are the high contents of amphoteric (Al_2O_3 and Fe_2O_3), acid (SiO_2) and alkali metal oxides (Na_2O and K_2O). It is therefore worthwhile to investigate to which extent red muds containing large quantities of amphoteric oxides. Fe_2O_3 and Al_2O_3 (over 60%) could be used as components of the alkali activated cements in long term applications.

More and more attention is paid to the presence of naturally occurring radionuclides in building materials. According to the CPR (Construction Products Regulation) the construction works must be designed and built in such a way that emission of dangerous radiation will not be a threat to health of occupants or neighbors. A unified legislation across the Member States of the European Union will come into act in February 2018 i.e. the Euratom Basic Safety Standards (EU-BSS, [CE-2014]). According to this legislation building materials incorporating naturally occurring radioactive materials (NORM), such as red mud, require a radiological screening before approved use as building materials. Red muds can contain enhanced concentrations of naturally occurring radionuclides [Somlai et al, 2008;Nuccetelli et al., 2015].

In this study different mixture designs were formulated that enable the incorporation of high percentages of red mud in cement and concrete. To assure safe application of red mud in the different considered mixtures, the radiological properties of the constituents and the resulting construction materials are investigated.

2. Materials and methods

2.1 Constituents

Concrete and cement specimens (d= 50 mm; h= 25 mm) with various incorporation rates of bauxite residue were prepared. The chemical composition of the main constituent materials used in the concrete and cement specimens are given in Table 1.

A Ukrainian red mud of the following mineralogical composition (% by mass): 25-27% hematite, 25-28% goethite, 4.5-6.5% rutile and anatase, 15-17% hydrogarnets, 6-7% sodium aluminosilicate hydrate, 2.5-3.0% calcite was used in the experiments in cements and concretes.

Blast-furnace slag and Ordinary Portland Cement (OPC) were used to introduce aluminosilicate components varying in basicity, expressed by a basicity modulus $\left(M_b = \frac{CaO + MgO}{SiO_2 + Al_2O_3} \right)$, and content of glass phase (80% for GGBFS and 5% for OPC measured by XRD analysis) in order to regulate the structure formation processes.

All solid cement constituents excluding alkalis were jointly ground until a fineness of 350-450 m²/kg (specific surface by Blaine).

Sodium silicate (Ms=2.8; p=1300 kg/m³); soda ash (Na₂CO₃) and sodium metasilicate pentahydrate (Na₂O·SiO₂·5H₂O) were used as alkaline components.

Local river sand with maximum grain size of 1.2 mm, granite aggregate with fractions 5-10 mm and 5-20 mm, granite screenings (fr. 2.5-5 mm) and red mud with particle sizes varying from 50 to 1000 μm were used as aggregates for concretes.

Table 1

Chemical composition of constituent materials

Cement components	Oxides, % by mass									
	SiO ₂	Al ₂ O ₃	MnO	Fe ₂ O ₃	CaO	MgO	TiO ₂	R ₂ O	M _b	Glass content
Red mud	4.8	12.9	-	48.6	10.1	-	5.3	2.5	-	-
Ground Granulated blast-furnace slag (ggbs)	37.9	6.85	0.106	-	44.6	5.21	0.35	-	1.0	80
OPC	23.4	5.17	-	4.12	64.13	0.88	-	-	2.27	5

2.2 High volume red mud alkali activated cements

Different compositions of red mud, ground granulated blast-furnace slag (glassy additive) and OPC (high-basic calcium containing additive) were mixed with soda ash, sodium metasilicate and soluble sodium silicate as alkaline components in order to produce alkali activated cements. An overview of the compositions of the produced alkali activated cements is given in Table 2.

Table 2

Compositions of alkali activated cements containing red mud

Composition	Red mud, % by mass	ggbs, % by mass	OPC, % by mass
Alkaline component: soda ash (Na ₂ CO ₃)(5% by mass of ggbs + red mud)			
K1	50	50	-
K2	60	30	10
K3	70	30	-
K4	70	20	10
K5	80	15	5
Alkaline component: sodium metasilicate (Na ₂ SiO ₃)(5% by mass of ggbs + red mud)			
K6	50	50	-
K7	70	25	5
Alkaline component: soluble sodium silicate (Ms=2.8, ρ=1400 kg/m ³) (soluble sodium silicate/ggbs + red mud=0.4)			
K8	50	50	-
Alkaline component: soluble sodium silicate (Ms=2.8, ρ=1300 kg/m ³) (soluble sodium silicate/ggbs + red mud=0.4)			
K9	60	30	10
K10	50	50	-

2.3 Red mud containing concretes

Different concentrations of red mud were used as fine aggregate in alkali activated cement concretes. For the concrete mixes given in table 3, fine aggregate – sand – was substituted for up to 38.6% (by mass) bauxite red mud.

Table 3

Characteristics of high volume red mud alkali activated cement concretes (quantities of red mud– up to 38.6% by mass of dry constituents)

No	Cement components, (kg)			Aggregates, (kg)	
	ggbs	OPC	alkaline component	crushed stone (fraction)	red mud
C1	536	14	soluble sodium silicate ($p=1400 \text{ kg/m}^3$, $M_s=2.8$), 308	800 (5-20)	850
C2	536	14	soluble sodium silicate ($p=1400 \text{ kg/m}^3$, $M_s=2.6$), 460	200 (5-10) 200 (screenings)	850

The concrete products listed in Table 4 are manufactured by pressing.

Table 4

Mix design of pressed (press stress $P=30 \text{ MPa}$) concrete road bases with various incorporation rates of red mud

No	Concrete mixture design, % by mass				
	Cement, % by mass			Aggregates, % by mass	
	ggbs	Na_2CO_3	$\text{Na}_2\text{SiO}_3 \cdot 5\text{H}_2\text{O}$	red mud	sand (fr. finer than 0.63 mm)
CRB1	13.8	0.6	0.6	85	-
CRB2	13.8	0.6	0.6	65	20
CRB3	13.8	0.6	0.6	45	40
CRB4	9.2	0.4	0.4	90	-

2.4 Methods for physico- mechanical analysis

Physico- mechanical properties of the formulated cements were studied following the Ukrainian national standard DSTU B.V 2.7-181:2009 “Alkaline cements. Specifications”. In the preparation of the concretes the Ukrainian national standard DSTU - N B.V.2.7-304:2015 “Manual on the manufacture and use of alkaline cements, concretes and structures” was followed. Specimens were allowed to harden in normal conditions.

Hydration products of the formulated cements were studied using a set of physico- chemical examination techniques, such as X-ray phase diffractometry, differential-thermal analysis (DTA), thermogravimetry and electron microscopy. X-ray phase diffraction analysis was done using diffractometers DRON-3M and DRON-4-07 with a copper tube at voltage=30 kV, current=10-20 mA and angle range $2\theta = 10-60^\circ$ at a speed of counter rotation= 2° per minute. Differential- thermal and thermogravimetric analyses were carried out using an instrument of the system F.Paulik, J.Paulik, L.Erdey (company MOM, Budapest, Hungary). The specimens were heated at a speed of 10°C per minute until a temperature of 1000°C was reached. Scanning electron microscopy (SEM) was carried out using scanning electron microscope

equipped with microanalyzers REMMA-102-02 (resolving power in the regime of secondary electrons is no more than 5 nm, magnification range is X10400000, a range of accelerating voltage of 0.2- 40 kV is used, maximum excessive pressure in the electron column is $6.7 \cdot 10^{-4}$ Pa).

Softening coefficient of material was calculated as a ratio between compressive strength after saturation in water for 2 days and compressive strength of reference material (not saturated). The material is water resistant if the softening coefficient is more than 0.8 [DSTU B A.1.1-5-94].

2.5 Method for radiological evaluation

The gamma-ray spectrometry measurements were performed on a HPGe-detector of the Radionuclide Metrology Laboratory of JRC-Geel in Belgium. The detector is located in the 225 m deep underground laboratory Hades located on the premises of the Belgian Nuclear Centre SCK•CEN in Mol, Belgium. The crystal has a planar configuration and a small point contact (so-called BEGe-detector). The relative efficiency is 19% and FWHM of 1.23 keV and 1.64 keV at respectively 661.6 keV and 1332 keV. It has a submicron top dead layer. The shielding is composed of 5 cm copper + 15 cm lead. The background count rate of the detector is 220 counts per day in the energy interval 40 to 2700 keV. All samples were dried at 110°C until constant mass was reached. Then they were placed in radon-tight Teflon containers and stored for at least 21 days before starting a measurement (to establish secular equilibrium between ^{226}Ra and daughters). The samples were placed directly on the endcap. The sample masses were 94.92 g, 134.74 g, 114.18 g and 138.85 g for ggbs, sand, OPC and red mud respectively. The measurement times varied between 7 and 17 days and the deadtime was always below 1%. All the activity concentrations are reported with the measurement date as reference date, which was between 395 and 440 days after the sampling date. No decay correction to the sampling date was made.

An activity concentration index (ACI_{SP}) for streets and playgrounds (Equation 1) that uses the activity concentrations of ^{226}Ra , ^{232}Th , ^{40}K and ^{137}Cs has been defined by Markkanen (1995),

$$ACI_{SP} = \frac{Ac_{226Ra}}{700 \frac{Bq}{kg}} + \frac{Ac_{232Th}}{500 \frac{Bq}{kg}} + \frac{Ac_{40K}}{8000 \frac{Bq}{kg}} + \frac{Ac_{137Cs}}{2000} \quad (1)$$

with Ac being the activity concentration of the mentioned radionuclide expressed in Bq/kg.

Note that an ACI_{SP} index value above 1 indicates an effective gamma dose larger than 0.1 mSv/a. The activity concentration index proposed by the EU-BSS could not be used in this case, since it was defined for evaluation of building materials and not for road construction.

In this study, the used activity concentration of ^{232}Th is the activity concentration of ^{228}Ac and the activity concentration of ^{226}Ra is the weighted mean between the activity concentrations of ^{214}Pb and ^{214}Bi . The ^{40}K and ^{137}Cs activity concentrations were measured directly using their respective gamma emission lines at 1460.8 keV and 661.6 keV.

Equation 2 is used for the calculation of the uncertainty (u) on the ACI_{SP} .

$$u(ACI_{SP}) = \sqrt{\left(\frac{1}{700}\right)^2 u^2(AC_{226Ra}) + \left(\frac{1}{500}\right)^2 u^2(AC_{232Th}) + \left(\frac{1}{8000}\right)^2 u^2(AC_{40K}) + \left(\frac{1}{2000}\right)^2 u^2(AC_{137Cs})}$$

(2)

With $u(AC_{226Ra})$ being the uncertainty on the activity concentration of the mentioned radionuclide.

Following Radiation Protection 122 (RP-122 part II, Chapter 4.2.6) dose assessments of road construction workers were performed such that it considers the occupational exposure linked to the use of concrete containing red mud. In this work, the NIRS (Japanese National institute on Radiological Sciences) dose assessment tool was used for the dose assessments calculations [NIRS website].

The activity concentration (in this paper meaning the activity per unit of mass) was determined by dividing the final activity determined for each radionuclide by the measured dry mass of the sample. The used methodology regarding the data analysis (data acquisition, spectrum analysis, full peak efficiency calculation), dose assessment and calculation of the ACI_{SP} is described in more detail in by Croymans et al. (2016).

3. Results and discussion

Several steps are undertaken for a systematic investigation of the use of high volume fractions of red mud in alkali activated cements and concretes:

(1) Firstly, the concept that enables the compositional buildup of alkali activated cement, using a high volume fraction of red mud, is proposed and a proof of concept is given.

(2) Secondly, the role of red mud in the structure formation of hardened cement paste is investigated in detail.

(3) Thirdly, the use of red mud as an aggregated in concrete for road base is evaluated.

(4) Finally, the radiological properties of the synthesized alkali activated cements and concretes are evaluated.

3.1 Concept for compositional buildup of alkali activated cement

The process of hydration and hardening can be considered as a complex process involving (1st stage) destruction-coagulation, (2nd stage) coagulation-condensation and (3rd stage) condensation-crystallization [Glukhovsky, 1994]. It was demonstrated that the quantity of glass phase is a determining factor at the 1st stage of the processes of hydration and hardening [Krivenko, 1985]. Crystalline high-basic calcium silicates quickly hydrate in alkaline medium promoting acceleration of the 3rd stage because of their hydration products. These calcium silicates can act as crystallo-chemical intensifiers of hardening. Absence of these crystalline phases in the initial material retards the 3rd stage of the structure formation process.

The role played by anions originating from alkaline component is a double one and is determined by the anion type. Anions can be divided into two groups: (1) anions that enter into cement within soluble silicates and aluminates and (2) anions that can be found in all remaining alkaline compounds. The anions of the first group are similar

to the hydrated primary destruction products of the aluminum-silicon-oxygen framework in the solid phase (SiOH), they serve as a reserve for the hydrated primary destruction products and, naturally, are the most effective anions in terms of hydration and structure formation. Anions of the second group change the properties of the liquid phase, and some participate in the formation of complexes which extract the destruction products into a solid phase promoting intensification of the hydration processes [Krivenko, 1985].

Thus, a compositional buildup of high volume red mud alkali activated cements should be based on a proper choice of the optimal ratio of red mud (with additives of glassy structure) to high-basic additives which quickly hydrate and crystallize in highly alkaline media [Krivenko, 1996, Rostovskaya, 1994].

In order to verify this concept in practice, a mixture of cement components containing 60% (by mass) ground bauxite red mud, 30% (by mass) granulated blast-furnace slag (glassy additive) and 10% (by mass) OPC (high-basic calcium containing additive) (K9 in Table 2), was mixed with soluble sodium silicate ($M_s=2.8$; $p=1300 \text{ kg/m}^3$). For the sodium silicate solution, the liquid to solid ratio was 0.4. The strength of the prepared cement-sand mortar (1:3) specimens was 6.25 MPa after 2 days of normal hardening (temperature $20\pm 2^\circ\text{C}$ and relative humidity $95\pm 4\%$), 30 MPa after 7 days and— 60 MPa after 28 days demonstrating that this concept can be used.

3.2 Role of red mud in the microstructure formation of hardened cement paste

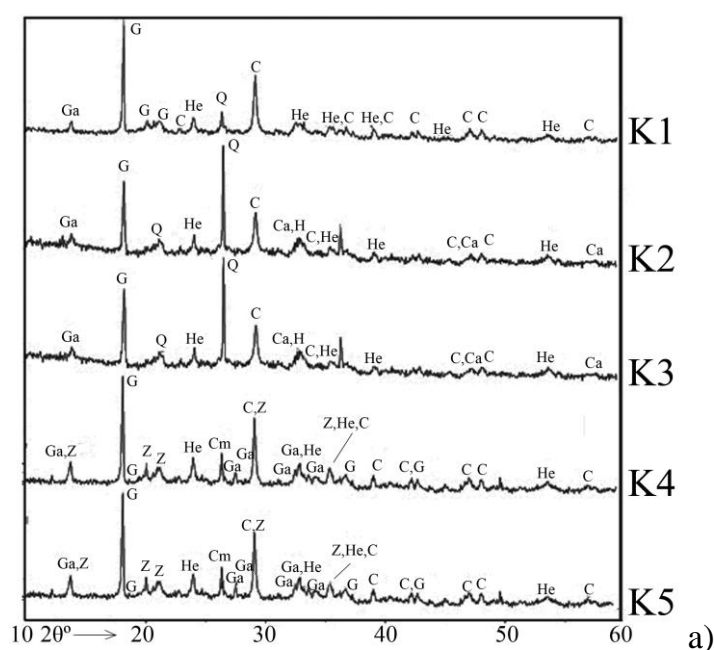
For the determination of the microstructure of the hardened cement paste the compositions in Table 2 were used. The role of red mud in the microstructure formation was investigated when using (1) soda ash, (2) sodium metasilicate and (3) sodium silicate as alkaline components.

The determination of the phase composition of hydration products of the formulated cements was not straightforward. This can be explained, from one side, by a multi-component composition of cementitious systems themselves, and from the other side, by the fact that each individual component is also a complex system (red mud, slag and cement). In some cases, this resulted in a superposition of characteristic responses making identification of the hydration products more complicated.

The results of X-ray phase diffraction analysis (Figure 1a) of the cements K1-K5 (Table 2) in which soda ash was used as alkaline component showed that hydration products were represented mainly by tri-calcium aluminates $3\text{CaO}\cdot\text{Al}_2\text{O}_3$ (diffraction characteristics 0.272; 0.191; 0.161, PDF#330251) and calcite CaCO_3 (0.368; 0.262; 0.228; 0.209; 0.191; 0.188, PDF#721937). The higher contents of the red mud in the cement composition (K5 and K4) resulted in the formation of zemkorite $\text{Na}_2\text{Ca}(\text{CO}_3)_2$ (0.639; 0.438; 0.425; 0.303, PDF#411440) and gaylussite $\text{Na}_2\text{Ca}(\text{CO}_3)_2\cdot 5\text{H}_2\text{O}$ (0.639; 0.270; 0.272; 0.321, PDF#210343). The addition of OPC (up to 10%) (K2, K4, and K5) was found to accelerate mineral formation processes at the early stages of hardening and improves the formation of a crystalline structure for the resulted cement stone.

In case of sodium metasilicate use (Figure 1b), the phase composition is somewhat different. The following minerals are formed: klinoferrosilite FeSiO_3 (0.643; 0.335; 0.321; 0.304; 0.260, PDF#821832) and lawsonite $\text{CaAl}_2[\text{Si}_2\text{O}_7](\text{OH})_2\cdot\text{H}_2\text{O}$ (0.487; 0.417; 0.368; 0.273, PDF#771994). When going to higher contents

of the red mud from 50 to 70% (K6 and K7) the structure formation process decelerates, though it does not stop completely. This means that the red mud takes an active part in cement hydration processes. The formation of clinoferrrosilite in the hydration products supports the assumption that hematite contained in large quantities in the red mud takes part, provides the condition of an alkaline medium, in the formation of hydration products. The use of soluble sodium silicate (K8) as alkaline component considerably accelerates the formation of calcium silicate hydrates and is a basement of crystallization processes in the cement. Soluble sodium silicate enters actively into interaction with red mud and calcium-containing additive. In the case of compositions with lower density of soluble glass (K9, K10) the prevailing hydration products are found to be tri-calcium aluminates $3\text{CaO}\cdot\text{Al}_2\text{O}_3$ (0.272; 0.191; 0.161, PDF#330251), calcites CaCO_3 (0.368; 0.262; 0.228; 0.209; 0.191; 0.188, PDF#411440) and crystals of hematite (PDF#850599).



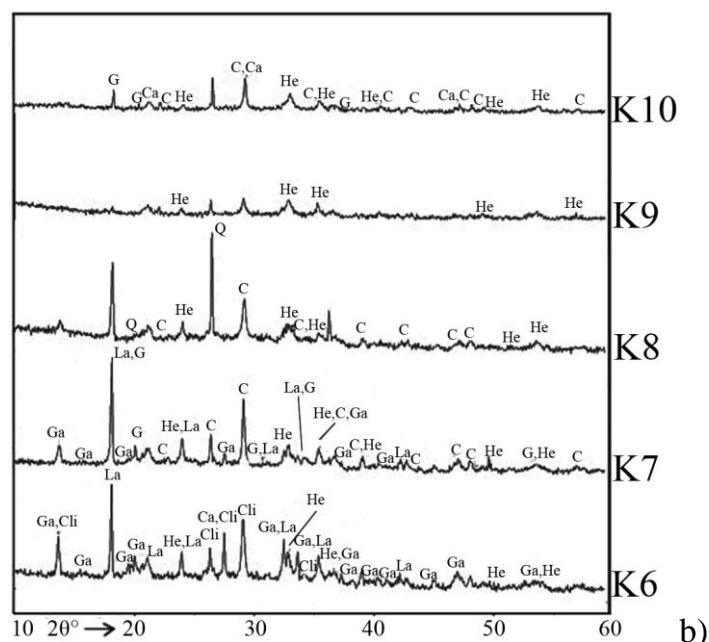


Fig.1. X-ray phase diffraction patterns of a cement stone from the alkali activated cements containing red mud and alkaline component: a – soda ash; b – soluble sodium silicate + sodium metasilicate. Designation: He – hematite (Fe_2O_3), Ca - $\text{Ca}_3\text{Al}_2\text{O}_6$ – tri-calcium aluminate ($3\text{CaO} \cdot \text{Al}_2\text{O}_3$), C – CaCO_3 – calcite, Q – (SiO_2) quartzite, G – gibbsite ($\text{Al}(\text{OH})_3$), Z – zemkorite ($\text{Na}_2\text{Ca}(\text{CO}_3)_2$), Ga – gaylussite ($\text{Na}_2\text{Ca}(\text{CO}_3)_2 \cdot 5\text{H}_2\text{O}$), Cm – caminite ($(\text{MgSO}_4)_2 \cdot (\text{OH})_2$), Cli – klinoferrosilite (FeSiO_3), La – lawsonite ($\text{CaAl}_2[\text{Si}_2\text{O}_7](\text{OH})_2 \cdot \text{H}_2\text{O}$)

The obtained results coincide well with the results of DTA. At temperatures between 270 and 350°C an endothermic effect takes place as a result of loss by gibbsite of OH^- groups. The occurrence of tri-calcium aluminate is confirmed by heat adsorption at 740°C (Figure 2) [Gorshkov et al., 1981]. A wide endothermic band in the DTA curve between 390 and 700°C gives an indication of the release of constitutional water with break of hydrogen bonds.

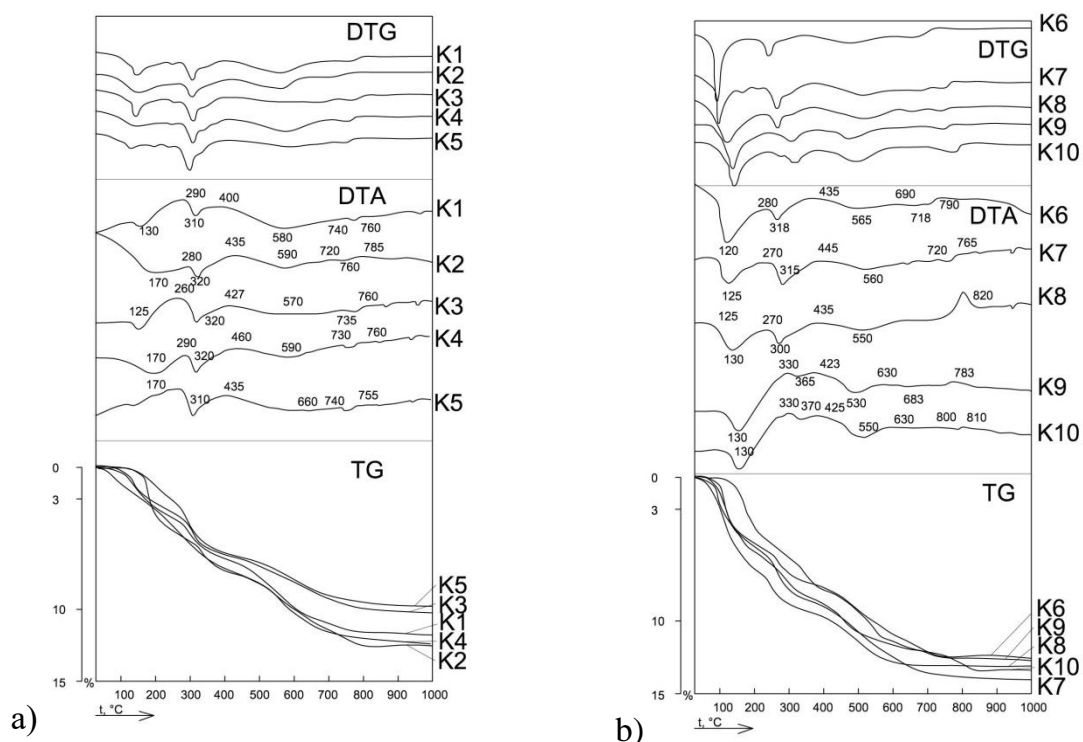


Fig. 2. DTA curves of a cement stone from alkali activated cement containing red mud and alkaline components: a – soda ash; b – soluble sodium silicate + sodium metasilicate

Electron microscopy studies of the cleavage surface of a cement stone from the alkali activated cement in case of soda ash as alkaline component showed the presence of calcium silicate hydrates, crystals of gaylussite (Ref to: <https://www.mindat.org/min-1662.html>) and particles of hematite (Ref to: <https://www.mindat.org/min-1856.html>) (Figure 3a, c). Photos taken of the cleavage surface case of sodium metasilicate, showed the formation of calcium silicate hydrates (Figure 3 b, d).

A cleavage surface featured a dense character without cracks, testifying to a uniform flow of the structure formation processes.

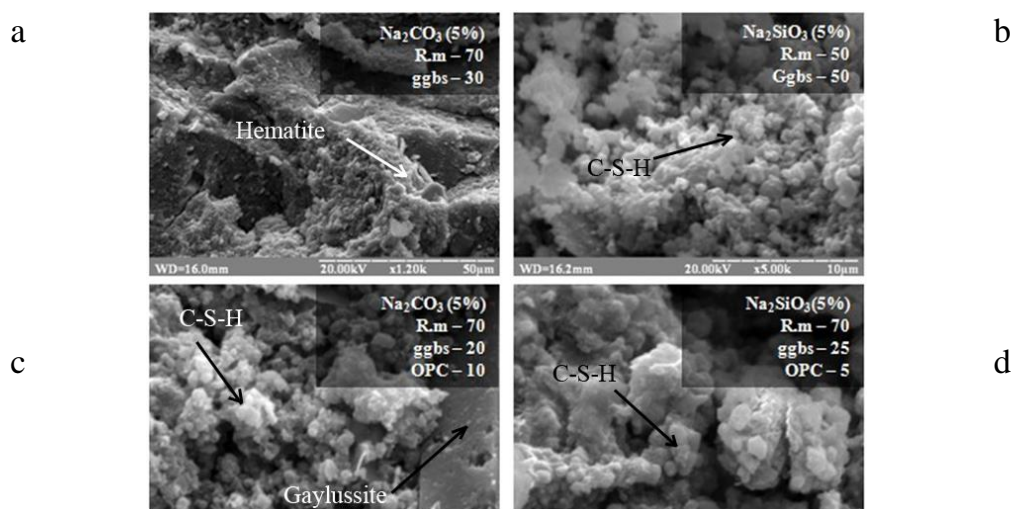


Fig.3. SEM images of the alkali activated cements with incorporated red mud, a – K3, b – K6, c – K4, d – K7

In case of soluble sodium silicate as alkaline component, the quantity of calcium silicate hydrates tends to increase considerably, testifying to a more active interaction of the components owing to the use of alkaline components with the higher silicate modulus.

At the same time, the formation of a gel-like phase of alkaline ferro-aluminosilicate hydrates could not be excluded [Locher F.W.]

3.3 High volume red mud alkali activated concrete mix design

Incorporation of red mud into alkali activated cement compositions, even in quantities reaching 60% by mass of the cement, will only lead to 14.5% by mass of red mud in the final product – concrete, under the assumption of a cement content of 500 kg/m³.

In order to increase the quantity of the incorporated bauxite residue, the red mud in a state “as produced” can be used as fine aggregates in making the alkali activated cement concretes. This type of concretes was produced and the concrete mix design is given in Table 3. Increasing of red mud content in the concrete mix (Table 3) to almost 40% by mass of concrete constituents leads to some problems at early stages of hardening. However, optimization of aggregate composition made it possible to have a good strength (over 20 MPa) even after 1 day. Results of the concrete test are given in Table 5.

Substitution of fine aggregate – sand – to up to 38.6% by mass red mud allows producing rather high-slump concretes with high strength reaching 70.8 MPa after 28 days (Table 5). Incorporation of even higher mass percentages of red mud in concrete mixtures can create technical difficulties because of its (red muds) high water demand as a result of the high fineness characteristic of red mud. The water content does not affect the concrete strength characteristics, however, it influences the performance properties of the resulted concretes leading to a lower freeze-thaw- and corrosion resistance.

Table 5

Characteristics of high volume red mud alkali activated cement concretes (quantities of red mud– reaching up to 38.6% by mass of dry constituents)

No	Slump (mm)	Compressive strength, (MPa), age		
		1 day	7 days	28 days
C1	170	13.72	43.57	63.5
C2	110	22.89	49.81	70.8

To tackle the issue of water demand, a possibility to utilize red mud in quantities in excess of 35% (by mass) is to use them in concrete products

manufactured by pressing (moisture content is 8-16% by mass).By means of pressing large percentages, up to 90% by mass, of red mud can be used when considering them for application in road base. The mix design of such materials is given in Table 4. Results of the study are given in Table 6.

Table 6 Characteristics of pressed (P= 30 MPa) concrete road bases with various incorporation rates of red mud

No	Water, % by mass over 100%	Density , kg/m ³	Compressive strength after 7 days, MPa
CRB1	15	2036	5.10
CRB2	14	2121	9.15
CRB3	12	2125	12.5
CRB4	16	2092	4.09

As is demonstrated by Table 6, even after seven days of hardening in normal conditions, the strength of the concrete was larger than 3.5 MPa, as is required for compressive strength of concrete road bases. Testing for water resistance showed that the specimen CRB 1, after 7 days of hardening in normal conditions and following 2 days of saturation with water, had a softening coefficient of 0.88 while specimen CRB 4 had a softening coefficient of 1.02. In this way, it is demonstrated that the materials are water resistant and from the technical point of view they could be used as a basis for road construction even when red mud incorporation is 90% by mass.

3.4 Radiological characterization

3.4.1 Radiological characterization of raw materials

In Table 7 the measured activity concentrations of the individual radionuclides in the main constituents of the red mud containing cements and concretes are given. The Minimum Detectable Activity (MDA) was determined using the decision threshold as defined in the standard ISO11929:2010.

Table 7

Measured activity concentrations in Bq/kg (dry weight) of individual gamma emitting radionuclides from the main constituents of the red mud containing concretes (k=2).

Sample	²³⁸ U series					²³⁵ U
	²³⁴ Th	^{234m} Pa	²¹⁴ Pb	²¹⁴ Bi	²¹⁰ Pb	²³⁵ U
Red mud	83 ± 17	84 ± 11	75 ± 5	73 ± 5	91 ± 19	3.5 ± 0.4
ggbs	103 ± 17	98 ± 13	99 ± 6	96 ± 6	<5	4.6 ± 0.4
OPC	36 ± 6	33 ± 5	32 ± 2	30 ± 2	22 ± 6	1.6 ± 0.2
Sand	2.6 ± 1.1	<10	3.0 ± 0.2	3.0 ± 0.3	2.9 ± 0.8	0.18 ± 0.04

Sample	²³² Th series					⁴⁰ K
	²²⁸ Ac	²²⁴ Ra	²¹² Pb	²¹² Bi	²⁰⁸ Tl	⁴⁰ K
Red mud	191 ± 12	188 ± 13	192 ± 13	189 ± 20	193 ± 12	39 ± 4
ggbbs	52 ± 4	53 ± 4	52 ± 4	49 ± 9	52 ± 4	119 ± 11
OPC	19.4 ± 1.5	18.5 ± 1.5	19.2 ± 1.3	18.0 ± 3.2	18.9 ± 2.0	231 ± 20
Sand	2.7 ± 0.3	2.8 ± 0.5	2.8 ± 0.2	<4	2.7 ± 0.3	64 ± 6

As we expect natural isotopic abundance, the values for ²³⁵U could be considered merely as a quality control tool. The activity ratio of ²³⁸U/²³⁵U is consistent within uncertainties with the expected value of 21.6 for all samples. When considering the ²³⁸U decay chain from ²³⁸U to ²¹⁴Bi, the activity concentrations of the different radionuclides in ggbbs are comparable or slightly higher in comparison to the same radionuclides in red mud (Table 7). The situation is different for ²¹⁰Pb. For ggbbs, there is no secular equilibrium anymore between ²¹⁰Pb and the other radionuclides in the ²³⁸U series whilst for red mud the equilibrium between ²³⁸U down to ²¹⁰Pb is maintained. Considering the production process of metallurgical slags, like ggbbs, it is reported in literature that the presence of volatile elements such as Pb is limited in the slag fraction [Croymans et al. 2017; European commission, 1997; Vanmarcke et al., 2003]. The activity concentrations of both red mud and ggbbs are 20-40 times higher than sand and 2-4 times higher than OPC for the measured radionuclides in the ²³⁸U decay chain (when not taking into account ²¹⁰Pb). Secular equilibrium is observed for both OPC and sand.

For the ²³²Th series, secular equilibrium is apparent from all the measured activity concentrations of the individual radionuclides in all four sample types (Table 7). The measured activity concentrations for the individual radionuclides in red mud are in this case approximately a factor 3.5 higher than the activity concentrations of the same radionuclides in ggbbs. For ⁴⁰K the activity concentration for ggbbs is a factor 3 higher than for red mud. When compared to sand, the activity concentrations of the radionuclides from the ²³²Th decay chain are approximately 70 and 19 times higher respectively for red mud and ggbbs. In comparison to OPC, the activity concentrations of respectively red mud and ggbbs are approximately a factor 10 and 3 higher for the ²³²Th decay chain.

¹³⁷Cs was not found in any of the samples and the MDA was in all cases below 1 Bq/kg.

3.4.2 Radiological evaluation of alkali activated cement pastes

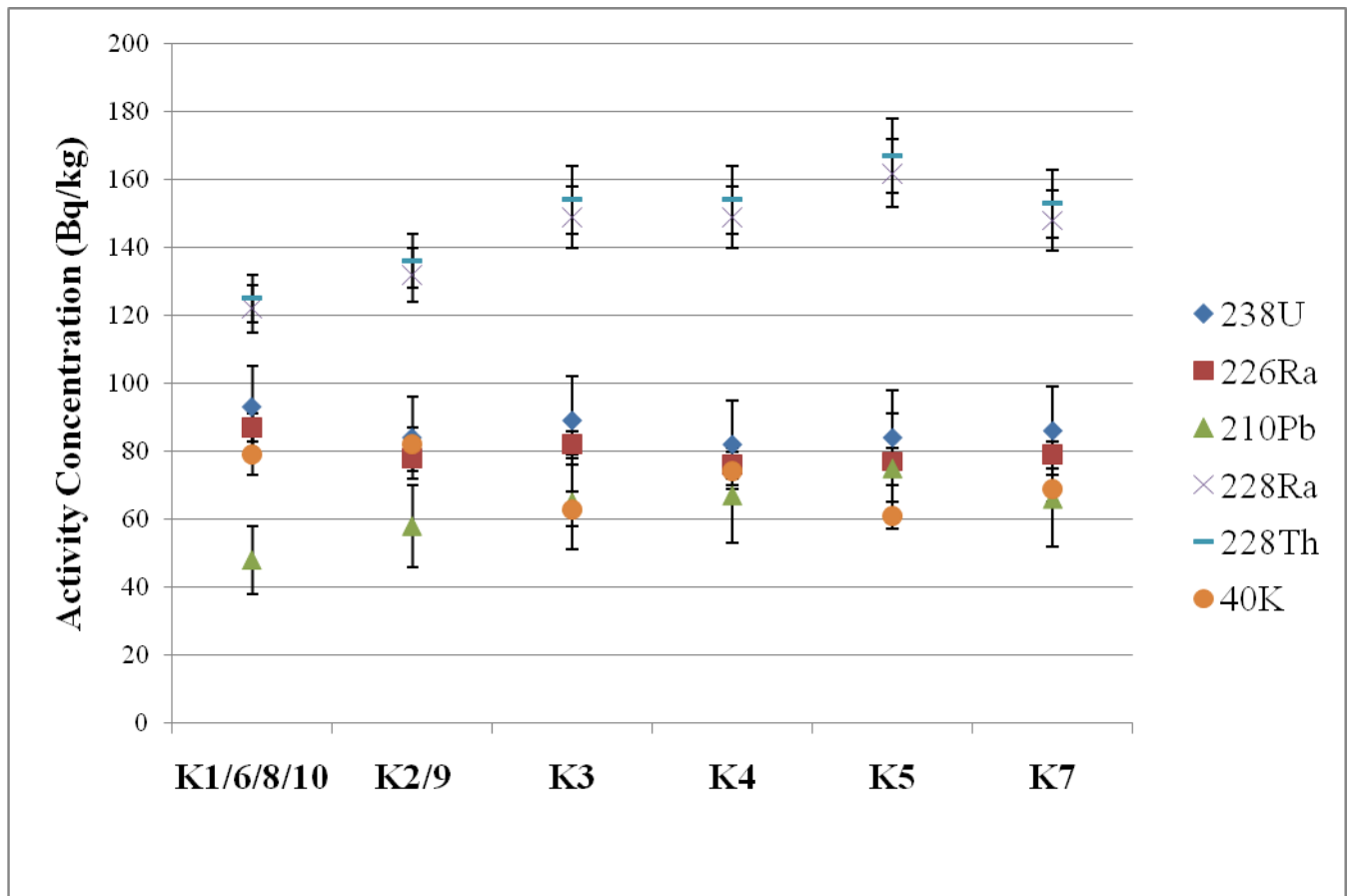


Fig. 4. Activity concentrations of the produced cements that were calculated on the basis of the measured activity concentrations of the constituents considering the composition in Table 2.

In Figure 4 the activity concentrations for the newly produced cements (composition in Table 2), calculated from the constituents, are given. For all the cements the activity concentrations of the considered radionuclides of the ^{238}U and ^{232}Th decay series and ^{40}K are well below the exemption/clearance levels of the EU-BSS of 1 kBq/kg and 10 kBq/kg.

3.4.3 Radiological evaluation of alkali activated concretes for road construction

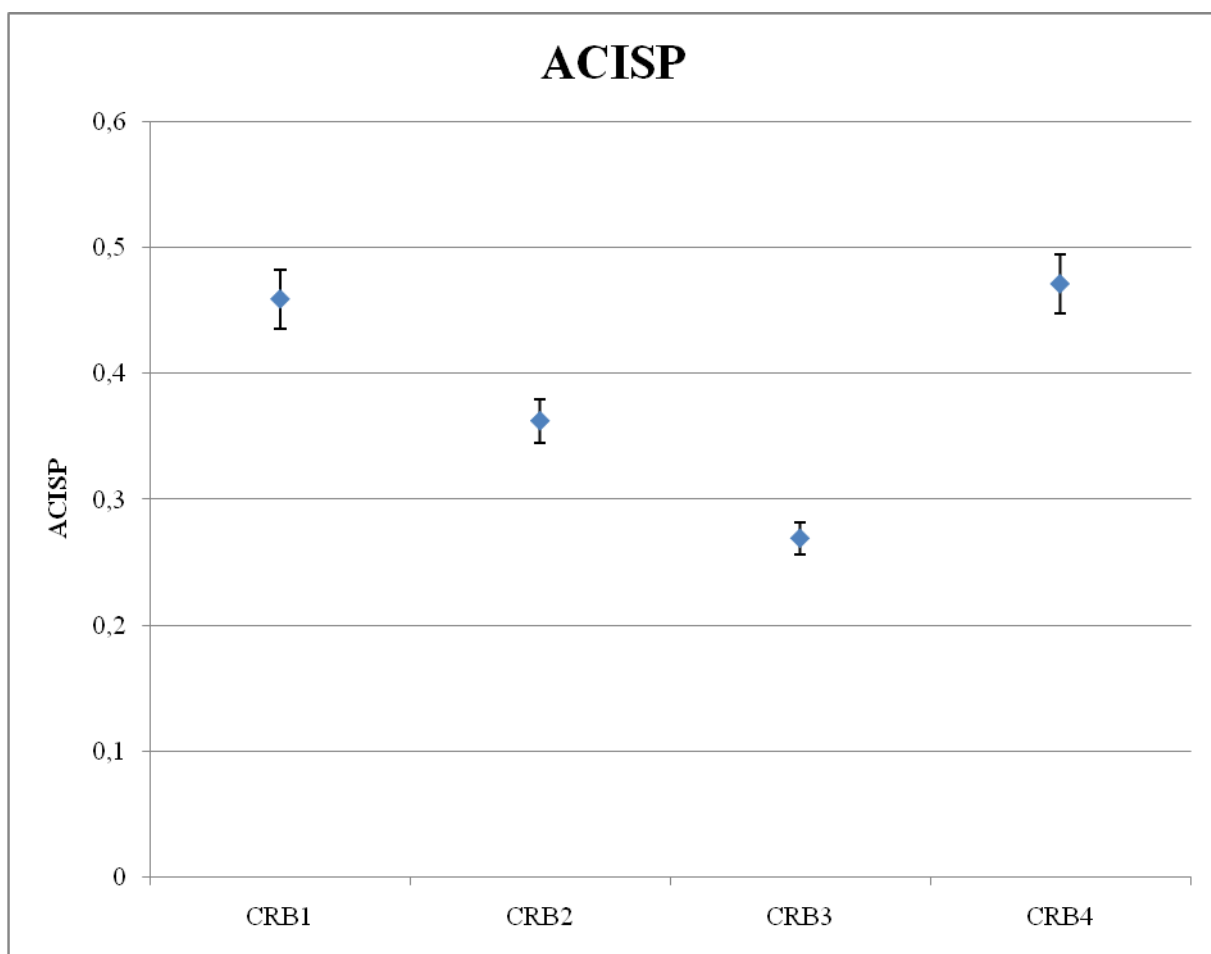


Fig. 5. $ACISP$ calculated for the produced concretes on the basis of the measured activity concentrations of the constituents considering the composition in Table 4.

The public and occupation exposure linked to the use of the prepared concrete mixtures (Table 4) for road base was verified. Figure 5 shows that all calculated $ACISP$ -values were below 1. So the external gamma dose for public exposure is lower than the 0.1 mSv/y dose threshold level proposed by Markkanen. The assessment of occupational exposure for workers - via the RP-122 part II “Road construction” scenario - was calculated for samples of Table 4. The calculated total doses to the road construction workers are 0.22 ± 0.02 ; 0.18 ± 0.02 ; 0.13 ± 0.01 and 0.23 ± 0.063 mSv/y for respectively CBR1, CBR2, CBR3 and CBR4. These values are below the 0.3 mSv/y dose threshold level proposed by RP-122 [European Commission, 2001].

4. Conclusions

The alkali activated cements with red mud incorporation reaching 80% by mass as well as concrete mixtures for road construction with incorporation rates reaching 90% by mass have been designed and tested. Compressive strength of cements could

reach up to 60 MPa and compressive strength of concrete could be up to 70 MPa depending on composition and technology.

Main hydration products explaining the high performance properties are: low-basic calcium silicate hydrates (CSH) and alkaline ferro- and aluminosilicate (kinoferrosilite FeSiO_3 , lawsonite $\text{CaAl}_2[\text{Si}_2\text{O}_7](\text{OH})_2 \cdot \text{H}_2\text{O}$).

From the radiological point of view all materials under study are able to be used for road construction, even when red mud incorporation reaches 90% by mass.

Acknowledgements

The authors would like to acknowledge networking support by the COST Action TU1301 (www.norm4building.org). This work was supported by the European Commission within HORIZON2020 via the EURATOM project EUFRAT for transnational access. The technical support of Gerd Marissens and Heiko Stroh is gratefully acknowledged.

References

- Bošković, I., Vukčević, M., Krgović, M., Ivanović M., Zejak, R. (2013), The influence of raw mixture and activators characteristics on red mud based geopolymers, *Research Journal of Chemistry and environment*, 17:34-40.
- CE - Council of the European Union, 2014. Council Directive 2013/59/EURATOM of 5 December 2013 laying down basic safety standards for protection against the dangers arising from exposure to ionizing radiation, and repealing Directives 89/618/Euratom, 90/641/Euratom, 96/29/Euratom, 97/43/Euratom and 2003/122/Euratom. Off. J. Eur. Union L 13, 1e73, 17.1.2014.
- Croymans, T., Schroeyers, W., Krivenko, P., Kovalchuk, O., Pasko, A., Hult, M., Marissens, G., Lutter, G., Schreurs, S. (2017), Radiological characterization and evaluation of high volume bauxite residue alkali activated concretes, *Journal of Environmental Radioactivity*, 168: 21-29.
- Croymans, T., Vandael-Schreurs, I., S., Hult, M., Marissens, G., Stroh, H., Lutter, G., Schreurs, S. Schroeyers, W. (2017), Variation of natural radionuclides in non-ferrous fayalite slags during a one-month production period, *J. Environ. Radioact.*, 172:63–73.
- Dimas, D.D.; Giannopoulou, I.P.; Panias, D. (2009), Utilization of alumina red mud for synthesis of inorganic polymeric materials. *Mineral Processing and Extractive Metallurgy Review: An International Journal*, 30:211-239.
- DSTU BA.1.1-5-94. General physical and technical characteristics and exploitation properties of building materials. Terms and definitions. (Ukrainian National Standard).
- European Commission (1997), Materials containing natural radionuclides in enhanced concentrations - Report EUR 17625.
- European Commission (2001), Radiation protection 122 practical use of the concepts of clearance and exemption Part II application of the concepts of exemption and clearance to natural radiation sources.

- Glukhovsky, V. (1994), Ancient, Modern and Future Concretes, First Inter. Conf. Alkaline Cements and Concretes. Ukraine, Kiev 1:1-8.
- Glukhovsky V.D. (1992), Selected works. Budivelnik, Kiev, Ukraine.
- Hairi, S.N.Md, Jameson, G.N.L., Rogers, J.J., MacKenzie, K.J.D. (2015), Synthesis and properties of inorganic polymers (geopolymers) derived from Bayer process residue (red mud) and bauxite, J.Mater. Sci. 50: 7713-7724.
- Gorshkov, V.S., Timashev V.V, Saveliev, V.G. (1981), Methods of chemical analysis of binders. Moscow
- Hajjajia W., Andrejkovičová A., Zanellic C., Alshaaerd M., Dondic M., Labrinchab J.A., Rochaa F. (2013), Composition and technological properties of geopolymers based on metakaolin and red mud. Materials & Design, 52:648-654.
- He J., Zhang Z., Yu Y., Zhang G. (2012), The strength and microstructure of two geopolymers derived from metakaolin and red mud-fly ash admixture: A comparative study. Construction and Building Materials, 30:80-91.
- He J, Jie Y, Zhang Z, Yu Y, Zhang G (2013), Synthesis and characterization of red mud and rice husk ash-based geopolymer composites. Cement and Concrete Composites, 37:108-118.
- Hertel, T., Blanpain, B. & Pontikes, Y. (2016), A Proposal for a 100 % Use of Bauxite Residue Towards Inorganic Polymer Mortar, J. Sustain. Metall., 2 (4):394-404
- Ke, X., Ye, N., Bernal, S.A., Provis J.L., Yang, J. (2014), Preparation of one-part geopolymer from thermal alkali activated bauxite red mud. Proc. Second Int. Conf. on Advances in Chemically-activated Materials. June 1-3, Changshi, P.R.China, 204– 211.
- Ke, X, Bernal S.A., Ye, N, Provis, L.J., Yang, J. (2015), One-Part Geopolymers Based on Thermally Treated Red Mud/NaOH Blends. J Am Ceram Soc, 98:5-11.
- Klauber, C., Gräfe, M., Power G. (2011), Bauxite residue issues: II. options for residue utilization. Hydrometallurgy, 108:11-32
- Komnitsas K, Zaharaki D (2009), Utilization of low-calcium slags to improve the strength and durability of geopolymers. Geopolymers: Structures, Processing, Properties and Industrial Applications. Woodhead, Cambridge, p.353.
- Krivenko P.V., (1985), Synthesis of Binders with Required Properties in the system $\text{Me}_2\text{O}-\text{MeO}-\text{MeO}_3-\text{SiO}_2-\text{H}_2\text{O}$. DSc(Eng.) Thesis, Kyiv, (in Ukraine)
- Kumar, A., Kumar, S. (2013), Development of paving blocks from synergistic use of red mud and fly ash using geopolymerization. Construction and Building Materials, 38:865-871.
- Liu, Z., Li, H. (2015), Metallurgical process for valuable elements recovery from red mud—A review, Hydrometallurgy, 155: 29-43
- Locher, F.W. (2006), Cement. Principles of production and use. Dusseldorf,
- Manfroi, E.P., Cheriaf, M., Rocha, J.C. (2014), Microstructure, mineralogy and environmental evaluation of cementitious composites produced with red mud waste. Constr. Build. Mater., 67, 29–36 (Part A).

- Markkanen, M. (1995), Radiation dose assessments for materials with elevated natural radioactivity. STUK-B-STO 32, Helsinki 1995. 25 p. + app. 13 p.
- NIRS database; NIRS, NORM database Research Center for radiation protection – National institute of radiological sciences. http://www.nirs.go.jp/db/anzendb/NORMDB/ENG/1_datasyousai.php consulted in March and April 2016
- Nuccetelli, C., Pontikes, Y., Leonardi, F., Trevisi, R. (2015), New perspectives and issues arising from the introduction of (NORM) residues in building materials: acritical assessment on the radiological behaviour. *Construction and Building Materials*, 82:323-331.
- Pan, Z., Dongxu, L., Jian, Y., Naunu, Y. (2003), Properties and microstructure of the hardened alkali-activated bauxite red mud slag cementitious material. *Cement and Concretes Research*, 33:1437– 1441.
- Pan, Z., Dongxu, L., Jian, Y., Nanru, Y. (2002), Hydration products of alkali-activated slag-bauxite red mud cementitious materials. *Cement and Concretes Research*, 32:357– 362.
- Pascual, J., Corpas, F., Lopez-Beceiro, J., Benitez-Guerrero, M., Artiaga, R. (2009), Thermal characterization of a Spanish bauxite red mud. *Journal of Thermal Analysis and Calorimetry*, 96(2):407– 412.
- Patent of Ukraine UA 10286 A, Krivenko P., Petropavlovsky O. Rostovskaya G., C 04 B7/06, 7/06, 25.12.96, Bulletin No 4.
- Pontikes, Y., Nikolopoulos, P., and Angelopoulos, G.N. (2007), Thermal behavior of clay mixtures with bauxite residue for the production of heavy clay ceramics. *Journal of the European Ceramic Society*, 27:1645–1649.
- Power, G., Grafe, M., and Klauber, C. (2009), Review of current bauxite residue management, disposal and storage: practices, engineering and science. CSIRO Document DMR-3608:3–4
- Rostovskaya, G.S. (1994), Alkaline binders based on bauxite residues. *First Int. Conference on Alkaline Cements and Concretes*, Kyiv, Ukraine, 1:329-346.
- Sglavo, V.M., Maurina, S., Conci, A., Salviati, A., Carturan, G., Cocco, G. (2000), Bauxite red mud in the ceramic industry Part 2: Production of clay-based ceramics. *Journal of the European Ceramic Society*, 20:245–252.
- Singh, M., Upadhyay, S.N., Prasad, P.M. (1997), Preparation of iron rich cements using red mud. *Cem. Concr. Res.*, 27(7):1037–1046.
- Somlai, J., Jobbágy, V., Kovács, J., Tarján, S., Kovács, T. (2008), Radiological aspects of the usability of red mud as building material additive. *Journal of Hazardous Materials*, 150(11):541-545
- Tsakiridis, P.E., Agatzini-Leonardou, S., and Oustadakis, P. (2004), Bauxite red mud addition in the raw meal for the production of Portland cement clinker. *Journal of Hazardous Materials*, 116:103– 110.
- Vanmarcke, H., Paridaens, J., Froment, P. (2003), Overzicht van de NORM-problematiek in de Belgische industrie. (in Dutch)
- Vukcevic, M., Turovic, D., Krgovic, M., Boscovic, I., Ivanovic, M., Zejak, R. (2013), Utilisation of Geopolymerisation For obtaining Construction Materials Based on Red Mud. *Mater Technol*, 47:99-104.

- Ye, N., Yang, J., Ke, X., Zhu, J., Li, Y., Xiang, C., Wang, H., Li, L., Xiao, B. (2014), Synthesis and characterization of geopolymer from Bayer red mud with thermal pretreatment. *J Am Ceram Soc*, 97:1652–1660.
- Zhang, G., He, J. and Gambrell, R.P. (2010), Synthesis, Characterization, and Mechanical Properties of Red Mud-Based Geopolymers, *Transportation Research Record: Journal of the Transportation Research Board*, 2167:1-9.
- Zhang, M., El-Korchi, T., Zhang, G., Liang, J., Mingjiang, T. (2014), Synthesis factors affecting mechanical properties, microstructure, and chemical composition of red mud–fly ash based geopolymers., *Fuel*, 134:315-325.